UKRAINIAN JOURNAL OF MECHANICAL ENGINEERING AND MATERIALS SCIENCE
Vol. 2, No. 1, 2016

Yuri Chovnyuk[1], Yuri Gumeniuk[1], Mykhailo Dikterjuk[2]
[1] National University of Life and Environmental Sciences of Ukraine, Kyiv, Ukraine
[2] Kyiv National University of Construction and Architecture, Kyiv, Ukraine

DYNAMIC MODELLING AND CONTROL SYSTEM OF A SINGLE NON-SLENDER FLEXIBLE ROBOT'S LINK ROTATING IN A HORIZONTAL PLANE

Received: June 6, 2016 / Revised: July 13, 2016 / Accepted: August 24, 2016

Abstract. Most authors have ignored the effect of rotatory inertia and shear deformation. This practice is justified for slender flexible arms. According to the Timoshenko beam theory, the deflection due to shear force and rotatory inertia should be taken into account in modelling for high speed and high precision requirement when the ratio of the cross-sectional dimensions to length increases.

Based on Hamilton's principle and Timoshenko's flexible beam theory, the dynamic model of a single non-slender flexible link is derived, and it is shown that the elastic motion is governed by a pair of coupled partial differential equations with coupled boundary conditions. Then the abstract form of the dynamic equations is studied, and the properties of the spectrum of the elastic operator appearing in the evolution equation are given. Furthermore, the eigenvalue problem of the elastic operator is solved in explicit form. The formulation and well-posedness of the state-space equation, as well as the transfer function of the dynamic control system of the non-slender flexible link, are studied by spectral analysis. Spectral analysis is used to study the well-posedness of the dynamic control system. The tracking control problem is studied and a feedback control scheme that controls the rigid-body motion and elastic behaviors simultaneously is derived based on a n-modal model. Closed-loop configuration of a control system, equivalent circuit of a dc-motor and the overall system block diagram are proposed. The stabilization of the closed-loop system is studied analytically.

Finally, the tracking control problem is studied, a stabilizing feedback control law based on a n-modal model to suppress vibrations of the flexible link is derived, and the necessary and sufficient conditions that can guarantee the stability of the closed-loop system, are given. Simulation results are given as well.

Introduction

Research in flexible robot arms has been conducted for several years. For example, Tzafestas and Kanoh [1], and Fukuda [2] presented excellent surveys on the modelling and dynamic control of flexible links. There have been numerous works on modelling and control of flexible arms, and various approaches have been presented. Some have given successful experimental studies (e.g. Sakawa et al. [3], Barbier and Özüner [4]). Most authors have ignored the effect of rotatory inertia and shear deformation. This practice is justified for slender flexible arms. According to the Timoshenko beam theory [5], the deflection due to shear force and rotatory inertia should be taken into account in modelling for high speed and high precision requirement when the ratio of the cross-sectional dimensions to length increases.

Earlier studies on the effect of shear flexibility and rotatory inertia on the bending vibrations of beams are presented by Traill-Nash and Collar [6]. New special attention has been given to the effect of rotatory inertia and shear flexibility on modelling and control of flexible robot links in [7, 8] and by Wang and Lu in [9]. Experimental analysis [8] showed that the errors due to neglecting the effect of rotatory inertia and of shear deformation become too significant to be tolerated for the inverse dynamic of non-slender flexible links. Our research was motivated by the efforts to give an analytical study of modelling and control of non-slender flexible links.

Firstly, based on Hamilton's principle and Timoshenko's flexible beam theory, the dynamic model of a single non-slender flexible link is derived, and it is shown that the elastic motion is governed by a pair of coupled partial differential equations with coupled boundary conditions. Then the abstract form of the dynamic equations is studied, and the properties of the spectrum of the elastic operator appearing in the evolution equation are given. Furthermore, the eigenvalue problem of the elastic operator is solved in explicit form. The formulation and well-posedness of the state-space equation, as well as the transfer function of the dynamic control system of the non-slender flexible link, are studied by spectral analysis. Finally, the tracking control problem is studied, a stabilizing feedback control law based on an n- model to suppress vibrations of the flexible link is derived, and the necessary and sufficient conditions that can guarantee the stability of the closed-loop system, are given. Simulation result are given as well.

Derivation of a dynamic model

As shown in Fig. 1, *a*, the system is made of a single non-slender flexible link that rotates in the horizontal plane. The rigid body motion and elastic behavior are controlled simultaneously by one dc-motor that is located at the point *O*. The payload at the fee and of the link is modelled as a concentrated mass *m*.

The coordinate changes employed are illustrated in Fig. 1, *b*. Let *X, Y, Z* designate the base coordinate system, where the *X,Y* axes span horizontal plane, and the *Z* axes is taken so that it coincides with the vertical rotation shaft of the motor. Let (*x, y, z*) denote the rotating coordinate system, and $q\left(t\right)$ be the rotation angle of the motor. In the rotating coordinate frame, let *w*(*x, t*) denote the deflection at point *x* and time *t*, and let $\Phi\left(s,t\right)$ be the slope of the deflection curve which is only due to the bending moment (see Fig. 1, *c*).

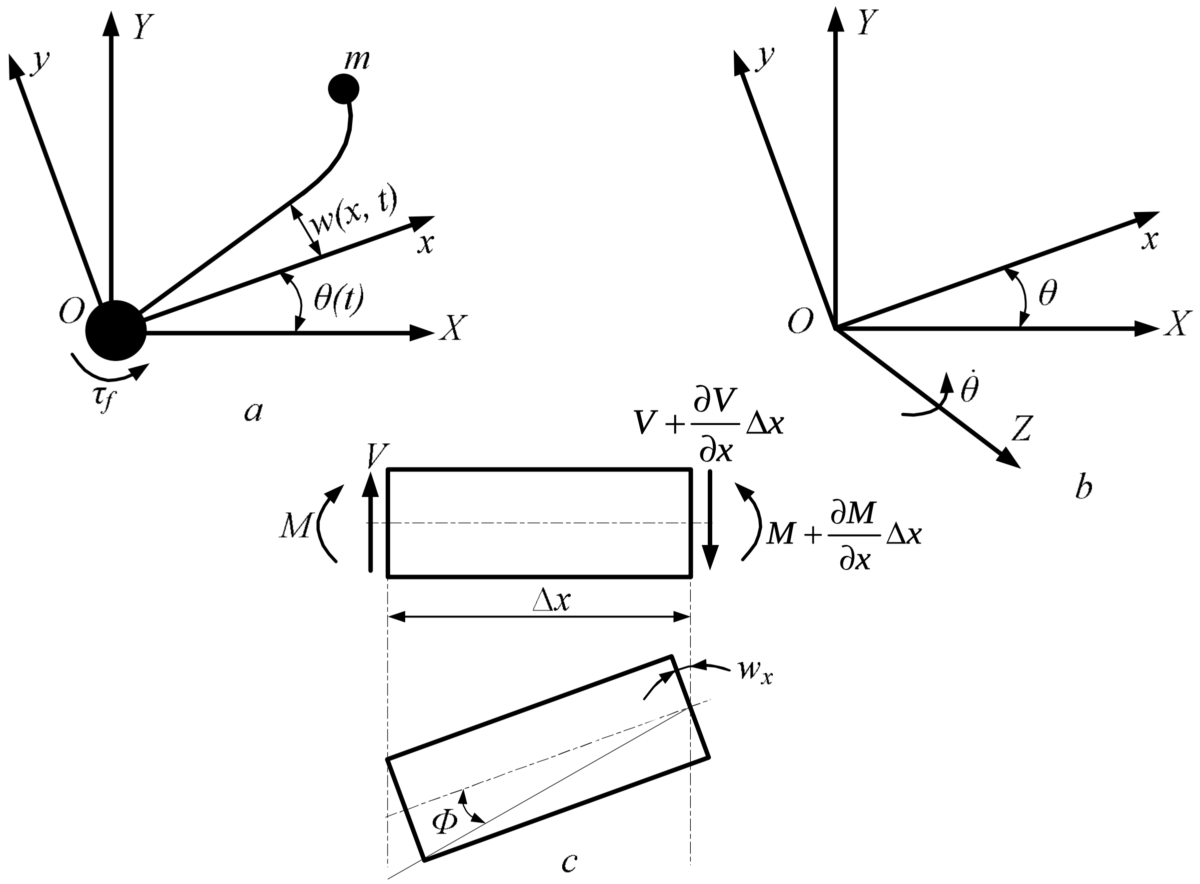

Fig. 1. *(a) Top view: the structure of a single flexible link;*
(b) the rotating coordinate frame; (c) force and moment balance

In order to establish the dynamic model of the single non-slender flexible link, we introduce Denavit-Hartenberg's description. Let *r* be the position vector with respect to the rotating coordinate frame; *r* is defined by the following homogeneous coordinate:

$$r = \left[x,\ w(x,t),\ 0,\ 1\right]^T . \tag{1}$$

Let *R* be the position vector with respect to the reference coordinate frame *X,Y,Z*. Thus $R = A \cdot r$, where *A* is the homogeneous coordinate transformation matrix, given by

$$A = \begin{bmatrix} \cos q & -\sin q & 0 & 0 \\ \sin q & \cos q & 0 & 0 \\ 0 & 0 & 1 & 0 \\ 0 & 0 & 0 & 1 \end{bmatrix}. \tag{2}$$

Inertia velocity is given by

$$\dot{R} = \left[\frac{\partial A}{\partial q}\right]\dot{q} + A \cdot \dot{r} = \left[-\left(x \cdot \dot{q} + \dot{w}\right)\sin q - \dot{q} w \cos q ; \left(x\dot{q} + \dot{w}\right)\cos q - -\dot{q} w \sin q ; 0 ; 0\right]. \tag{3}$$

Ignoring the high order non-linear term $\dot{q} w$ in (3), gives

$$\dot{R} = \left[-\left(x \cdot \dot{q} + \dot{w}\right)\sin q ; \left(x\dot{q} + \dot{w}\right)\cos q ; 0 ; 0\right]^T . \tag{4}$$

In this paper, we assume that flexible link shown in Fig 1 is a uniform beam of length *l*, and mass per unit length, r . The mass moment of the rectangular cross section I_r is given by $I_r = r\,k^2$, where *k* is the radius of gyration of the link section, given by $k = d^2 / 12$, and *d* is the thickness of the link. *E* and *I* are Young's modulus and the moment of inertia of the cross-section, respectively; $C = [K \cdot G \cdot A]$ is the shear stiffness, where *G* is the modulus of elasticity in shear, *A* is the cross-sectional area and *K* is a numerical factor that depends on the share of the cross-section. Here the internal viscous damping of Kelvin-Voigt type is considered in the modelling. Let $h > 0$ be a small damping constant of the link material.

According to Timoshenko's theory [5] the bending moment *M* and shear force *V* can be represented as $M = EI\frac{\partial \Phi}{\partial x} + hEI\frac{\partial \Phi}{\partial x}$, $V = -C(\Phi - w_x) - h\,C(\dot{\Phi} - \dot{w}_x)$. The dynamic model of the non-slender flexible link is derived using Hamilton's principle as the following procedure. In fact, the kinetic energy is given by

$$K_e = \frac{1}{2} r \int_0^l \left(\dot{R}^T \dot{R}\right) dx + \frac{1}{2} r k^2 \int_0^l \left(\dot{\Phi} + \dot{q}\right)^2 dx + \frac{1}{2} I_h \dot{q} + \frac{1}{2}\left(m\dot{R}(l)^T \dot{R}(l)\right) + \frac{1}{2} m k^2 \left(\dot{\Phi}(l,t) + \dot{q}\right)^2 . \tag{5}$$

where I_h is the moment of inertia of the hub. The potential energy due to elastic deformation is given by

$$P_e = \frac{1}{2}\int_0^l \left\{EI\Phi_x^2 + C\left(\Phi - w_x\right)^2\right\} dx . \tag{6}$$

Hamilton's principle can be expressed as

$$\int_{t_1}^{t_2} d\left(K_e - P_e + W\right) dt = 0 , \tag{7}$$

where *W* is the work done by the non-conservative force, expressed as

$$dW = t_f\, d q + \int_0^l h C\left(\dot{\Phi} - \dot{w}_x\right) d\left(w_x - \Phi\right) dx - \int_0^l h EI \dot{\Phi}_x\, d\Phi_x\, dx , \tag{8}$$

and t_f is torque applied to the link. Substituting (5), (6) and (8) into (7) gives

$$I_h\ddot{q} = EI\;\Phi_x(0) + hEI\dot{\Phi}_x(0) + t_f\,, \tag{9}$$

and

$$\begin{cases} r\ddot{w} + C(\Phi_x - w_{xx}) + hC(\dot{\Phi}_x - \dot{w}_{xx}) = -r\,x\ddot{q}, \\ r\,k^2 + C(\Phi - w_x) + hC(\dot{\Phi} - \dot{w}_x) - EI\Phi_{xx} - hEI\dot{\Phi}_{xx} = -r\,k^2\ddot{q}, \end{cases} \tag{10}$$

with the boundary conditions

$$\begin{cases} w(0) = 0, \;\; \Phi(0) = 0; \\ m\left(l\ddot{q} + \ddot{w}(l)\right) = C(\Phi - w_x)(l) + hC(\dot{\Phi} - \dot{w}_x)(l); \\ mk^2\left(\ddot{q} + \ddot{\Phi}(l)\right) = -EI\Phi_x(l) - hEI\dot{\Phi}_x(l). \end{cases} \tag{11}$$

The mathematical aspects of the above dynamic equations are studied in the next section. With negligible armature inductance, the dc-motor is modelled by

$$I_m\ddot{q} + m\dot{q} + t_f = t\,, \tag{12}$$

where I_m is the moment of inertia of the motor, m is the viscous friction coefficient and t is the torque supplied by the motor.

Evolution equation

The hybrid system (9), (10) with the boundary conditions (11) represents the results of the physically reasoned derivation of the basic dynamic model utilized below. In this section, we treat the boundary value problem governed by (10), (11) as a distributed parameter system that is in the form of an abstract second order evolution equation in Hilbert space *H* defined by

$$H = L^2(0,l)\cdot L^2(0,l)\cdot R^2\,, \tag{13}$$

with the inner product

$$\left\langle [u_1;u_2;u_3;u_4],[v_1;v_2;v_3;v_4]\right\rangle_H = \int_0^l\left(r\,u_1v_1 + r\,k^2u_2v_2\right)dx + mu_3v_3 + mk^2u_4v_4\,, \tag{14}$$

where we take

$$u_1 = w(t,\cdot), u_2 = \Phi(t,\cdot), u_3 = w(t,\cdot l), u_4 = \Phi(t,\cdot l)\,.$$

Let *V* be a subspace of *H*, defined by

$$V = \left\{[u_1;u_2;u_3;u_4]\in H \left| \begin{array}{l} u_1(\cdot)\in H^1(0,l),\; u_2(\cdot)\in H^1(0,l)\,, \\ u_3 = u_1(l), u_4 = u_2(l),\; u_1(0) = 0,\; u_2(0) = 0 \end{array}\right.\right\}, \tag{15}$$

with the inner product

$$\left\langle [u_1;u_2;u_3;u_4],[v_1;v_2;v_3;v_4]\right\rangle_V = \int_0^l\left(u_1'v_1' + u_2'v_2'\right)dx + u_3v_3 + u_4v_4\,, \tag{16}$$

where the symbol (′) indicates the partial derivative with respect to *x* and $H^1(0,l)$ denotes a Sobolev space.

Define the operator *A* by

$$an = \left[\frac{c}{r}\left(u_2' - u_1'\right); \frac{c}{r\,k^2}\left(u_2 - u_1'\right) - \frac{EI}{r\,k^2}u_2''; \frac{c}{m}\left(u_4 - u_3'\right); \frac{EI}{mk^2}u_4'\right],$$
$$\forall u\in D(A) = \left\{u\in V \left| u_1'(\cdot)\in H^1(0,l), u_2'(\cdot)\in H^2(0,l)\right.\right\}, \tag{17}$$

where $D(A)$ denotes the domain of *A*.

Let Ω be a vector defined by

$$\Omega = -\left[x1l1\right]^T . \tag{18}$$

Thus the partial differential equations (10) with the boundary condition (11) can be rewritten in the following abstract form

$$\ddot{u}(t) + h\,A\dot{u}(t) + Au(t) = \Omega\ddot{q}(t) , \tag{19}$$

where $u(t) \in D(A) \subset V \subset H$.

For the elastic operator *A,* we obtain the following properties:

1. The operator *A* defined by (17) is a densely defined, self-ad-joint positive operator, and has a compact inverse operator A^{-1}.

2. *A* is closed operator with countable many eigenvalues $\{\lambda_n\}_{n=1}^{\infty}$ and corresponding generalized eigenvectors $\{\Psi\}_{i=1,\ j=1}^{m_j,\ \infty}$ that satisfy the following conditions:

a) $0 < l_1 < \lambda_2 < \ldots < \ldots ,\ \lim_{n\to\infty} \lambda_n = \infty$,

b) $A\Psi_{ij} = \lambda_i \Psi_{ij}, i = 1,2,\ldots,m_j, m_j < \infty, j = 1,2,\ldots,\infty$,

c) the set $\left\{\Psi_{ij}(\cdot)\right\}$ of the eigenvectors forms a complete orthonormal system in *H,* and

$$u(\cdot) = \sum_{i=1}^{\infty}\sum_{j=1}^{m_i} < u,\ \Psi_{ij} >_H \Psi_{ij}(\cdot), \forall u \in H . \tag{20}$$

The eigenvalue problem of *A* is solved in the next section.

Eigenvalue problem

From the property (b) of the second property for the elastic operator *A,* we see that

$$A\Psi = l\Psi , \tag{21}$$

where l is an eigenvalue of the operator *A* and $\Psi \in D(A)$ is the corresponding eigenvector. With the definition of *A,* can be rewritten in the following form:

$$\frac{c}{r}\left(\Phi_x - w_{xx}\right) = l\,w , \tag{22a}$$

$$\frac{c}{r k^2}\left(\Phi_x - w_{xx}\right) - \frac{B}{r k^2}\Phi_{xx} = l\Phi , \tag{22b}$$

$$\frac{c}{m}\left(\Phi - w_x\right)(l) = l\,w(l) , \tag{22c}$$

$$\frac{B}{mk^2}\Phi_x(l) = l\Phi(l) , \tag{22d}$$

$$w(0) = 0,\ \ \Phi(0) = 0 , \tag{22e}$$

where $B = EI$. It is convenient to write (22) in dimensionless form. Therefore we define $\bar{x} = x/l, \bar{w}(\bar{x}) = w(x)/l, \bar{\Phi}(\bar{x}) = \Phi(x)$, and introduce a new function *v* defined by

$$v = \bar{\Phi} - \bar{w}_x(\bar{x}) . \tag{23}$$

It is easily verified that *v* satisfies the following ordinary differential equation:

$$v^{(n)} + w^2(a + b)v^{(2)} - w^2\left(1 - w^2 ab\right)v = 0 , \tag{24}$$

where $v^{(n)}$ indicates the nth partial derivative with respect to *x,* and w, a, b are defined by

$$w^2 = \frac{r l^4 l}{B},\ \ a = \frac{B}{Cl^2},\ \ b = \frac{k^2}{l^2} . \tag{25}$$

The parameters w, a and b have the following important practical meanings: w is the natural frequency of vibration; a is proportional to flexibility; b is proportional to rotatory inertia.

In the remainder of this section we still write $\overline{x}$ as x for simplicity. The general solution of (24) is given by:

$$v(x)=\begin{cases} c_1 \sin px + c_2 \cos px + c_3 \sin qx + c_4 \cos qx, w^2 ab > 1; \\ c_1 \sin px + c_2 \cos px + c_3 \sin hrx + c_4 \cos hrx, w^2 ab < 1, \end{cases} \tag{26}$$

where $c_i, i = 1,\ldots,4$ are constants determined by (22c) – (22e) and

$$\begin{cases} 2p^2 = w^2(a+b) + \left[w^4(a-b)^2 + 4w^2\right]^{1/2}; \\ 2q^2 = w^2(a+b) - \left[w^4(a-b)^2 + 4w^2\right]^{1/2}; \\ r^2 = -q^2. \end{cases} \tag{27}$$

Using (23) and the boundary condition (22e), we have the following relationship:

$$\begin{cases} c_1 p + c_3 q = 0,\ c_2 \hat{p}^2 + c_4 \hat{q}^2 = 0,\ w^2 ab > 1; \\ c_1 p + c_3 r = 0,\ c_2 \hat{p}^2 + c_4 \hat{q}^2 = 0,\ w^2 ab < 1, \end{cases} \tag{28}$$

where $\hat{p}^2$ and $\hat{q}^2$ are defined by

$$\begin{cases} 2\hat{p}^2 = w^2(a-b) - \left[w^4(a-b)^2 + 4w^2\right]^{1/2}, \\ 2\hat{q}^2 = w^2(a-b) + \left[w^4(a-b)^2 + 4w^2\right]^{1/2}. \end{cases} \tag{29}$$

It’s not difficult to verify the following relationship using (22c, d) and (28)

$$\begin{bmatrix} a_{11}(w) & a_{12}(w) \\ a_{21}(w) & a_{22}(w) \end{bmatrix} \begin{bmatrix} c_1 \\ c_2 \end{bmatrix} = 0, \tag{30}$$

where

$$a_{11}(w)=\begin{cases} \sin p - \dfrac{p}{q}\sin q + \dfrac{pm}{lr}(\cos p - \cos q), w^2 ab > 1; \\ \sin p - \dfrac{p}{r}\sin hr + \dfrac{pm}{lr}(\cos p - \cos hq), w^2 ab < 1. \end{cases} \tag{31}$$

$$a_{12}(w)=\begin{cases} \cos p - \dfrac{\hat{p}^2}{\hat{q}^2}\cos q - \dfrac{m}{lr}\left(p\sin p - \hat{p}^2 \dfrac{q}{\hat{q}^2}\sin q\right), w^2 ab > 1; \\ \cos p - \dfrac{\hat{p}^2}{\hat{q}^2}\cos hr - \dfrac{m}{lr}\left(p\sin p + \dfrac{\hat{p}^2 r}{\hat{q}^2}\sin hr\right), w^2 ab < 1. \end{cases} \tag{32}$$

$$a_{21}(w)=\begin{cases} p\left(\hat{p}^2 \cos p - \hat{q}^2 \cos q\right) - \dfrac{w^2 bm}{lr}\left(\hat{p}^2 \sin p - p\dfrac{\hat{q}^2}{q}\sin q\right), w^2 ab > 1; \\ p\left(\hat{p}^2 \cos p\right) - \hat{q}^2 \cos hr - \dfrac{w^2 bm}{lr}\left(\hat{p}^2 \sin p + \dfrac{\hat{q}^2}{r}\sin hr\right), w^2 ab < 1. \end{cases} \tag{33}$$

$$a_{22}(w)=\begin{cases}\hat{p}^2(-p\sin p+q\sin q)-\dfrac{w^2bm}{lr}\hat{p}^2(\cos p-\cos q), w^2ab>1;\\ \hat{p}^2(-p\sin p-r\sin hr)-\dfrac{w^2bm}{lr}\hat{p}^2(\cos p-\cos hr), w^2ab<1.\end{cases} \tag{34}$$

Consequently, the characteristic equation is given by

$$a_{11}(w)a_{22}(w)-a_{21}(w)a_{12}(w)=0\,. \tag{35}$$

In the case where $w^2ab>1$ can be expressed in the following explicit form:

$$\begin{aligned}&-2\left(1+\frac{w^2bm}{lr}\right)+\left(2\frac{w^2bm}{lr}-w^2(a-b)-2\right)\cos p\cos q+w^2(a+b)+\\&+\left\{w^2(a+b)-b\frac{m^2}{r^2}\left[w^6(a-b)^2a+w^4(3a-b)\right]\right\}\frac{\sin p}{p}\cdot\frac{\sin q}{q}+\\&+\frac{m}{r}\left\{p^2\left[w^2(a--b)^2+4\right]-\left[w^4(a-b)^2+4w^2\right]^{1/2}\right\}\frac{\sin p}{p}\cdot\cos q+\\&+\frac{m}{r}\left\{q^2\left[w^2(a-b)^2+4\right]++\left[w^4(a-b)^2+4w^2\right]^{1/2}\right\}\cos p\cdot\frac{\sin q}{q}=0.\end{aligned} \tag{36}$$

Let $w_n^{(1)}$ and $w_n^{(2)}$ be the solution of (35) such that

$$0<\omega_1^{(1)}<\omega_2^{(1)}<\ldots<\omega_N^{(1)}<\left(\frac{1}{ab}\right)^{1/2}<\omega_1^{(2)}<\omega_2^{(2)}<\ldots<\lim_{n\to\infty}w_n^{(2)}=\infty\,.$$

Then for every $n\geq 1$, the eigenvalue λ_n of A is given by

$$\lambda_n=\frac{b}{rl^2}\omega_n^2\,, \tag{37}$$

where ω_n is defined by

$$\omega_n=\begin{cases}\omega_n^{(1)}, n\leq N,\\ \omega_{N-n}^{(2)}, n>N.\end{cases} \tag{38}$$

The corresponding eigenvector $\Psi_n=\left(w_n(\cdot),\Phi_n(\cdot),w_n(l),\Phi_n(l)\right)^T$ can be easily determined by

$$w_n(x)=\begin{cases}\dfrac{l}{\omega_n^2a}\left(c_1p_n\cos\dfrac{p_n}{l}x+c_2p_n\sin\dfrac{p_n}{l}x-p_n\cos\dfrac{q_n}{l}x-c_2\dfrac{\hat{p}^2n}{\hat{q}^2n}\sin\dfrac{q_n}{l}x\right),\omega_n^2ab>1;\\ \dfrac{l}{\omega_n^2a}\left(c_1p_n\cos\dfrac{p_n}{l}x+c_2p_n\sin\dfrac{p_n}{l}x-p_n\cosh\dfrac{r_n}{l}x-c_2\dfrac{\hat{p}^2nr_n}{\hat{q}^2n}\sinh\dfrac{r_n}{l}x\right),\omega_n^2ab<1.\end{cases} \tag{39}$$

$$\Phi_n(x)=\begin{cases}\dfrac{1}{\omega_n^2a}\hat{p}_n^2\left(c_1\sin\dfrac{p_n}{l}x+c_2\cos\dfrac{p_n}{l}x\right)+\\ +\dfrac{1}{\omega_n^2a}\left(-\dfrac{p_n}{q_n}\hat{q}_n^2c_1\sin\dfrac{q}{l}x+\hat{p}_n^2c_2\cos\dfrac{q}{l}x\right),\omega_n^2ab>1;\\ \dfrac{1}{\omega_n^2a}\hat{p}_n^2\left(c_1\sin\dfrac{p_n}{l}x+c_2\cos\dfrac{p_n}{l}x\right)+\\ +\dfrac{1}{\omega_n^2a}\left(-\dfrac{p_n}{q_n}\hat{q}_n^2c_1\sinh\dfrac{r}{l}x+\hat{p}_n^2c_2\cosh\dfrac{r}{l}x\right),\omega_n^2ab<1.\end{cases} \tag{40}$$

It c_1 and c_2, satisfy the relations in (28), are chosen so that $\left\|\Psi_n(\cdot)\right\|_H = 1$, then we obtain a set of orthonormalized eigenvectors.

From (36) it's easily seen that, when $n \to \infty, \omega_n^2$, tends to satisfy

$$\sin p_n \cdot \sin q_n = 0, \tag{41}$$

which is obtained by dividing both side of (36) by ω_n^4 and by letting $n \to \infty$. Thus for large values of *n*, we see that

$$\omega_n^2 \sim O\left(n^2\right). \tag{42}$$

The case where $\omega^2 = \dfrac{1}{ab}$ is specially treated as follows. In this case, the general solution of (24) is $v(x) = c_1 + c_2 x + c_3 \sin \bar{p}x + c_4 \cos \bar{p}x$ where $\bar{p}^2 = w^2 (a + b)$, and then the eigenvector corresponding to $w^2 = \dfrac{1}{ab}$ is given by

$$\begin{aligned} w(x) &= \frac{1}{w^2 a}\left\{\bar{p}c_3\left(-1+\cos\frac{\bar{p}}{l}x\right) - \bar{p}c_4 \sin\frac{\bar{p}}{l}x\right\}, \\ \Phi(x) &= \frac{b}{a}c_4\left(1-\cos\frac{\bar{p}}{l}x\right) - c_3\left(\bar{p}+\frac{b}{l}\sin\frac{\bar{p}}{l}x\right), \end{aligned} \tag{43}$$

where $c_1, c_{2,} c_3$ and c_4 satisfy the following relations: $c_1 = \dfrac{b}{a}c_4$, $c_2 = \bar{p}c_3$, $b_1 c_3 + b_2 c_4 = 0$ and $b_1 = \left(-\bar{p} + \sin \bar{p}\right) + \dfrac{m}{lr}\left(-1 - \cos \bar{p}\right)\bar{p}$, $b_2 = \left(\dfrac{b}{a} + + \cos \bar{p}\right) - \dfrac{m}{lr}\bar{p}\sin \bar{p}$ and c_3 and c_4 are chosen so that Ψ has unit norm.

Control system

In this section, we consider the tracking control problem of the end-point position of the non-slender flexible link discussed in the previous sections. We assume that the output of the control system of the flexible link is obtained by a strain gauge attached at the link at $x = 0$, which can be expressed as $y(t) = \Phi'(t, 0)$ i.e. the bending moment at $x = 0$ is measured.

Formulation and well-posedness

Firstly, we recall two types of definitions of the formulation of linear infinite-dimensional systems state-space description (Pritchard-Salamon class) and frequency domain description (Callier-Desoer class), which have been developed for the control theory of infinite-dimensional systems, and which are relevant to our present study.

Pritchard-Salamon class (Pritchard and Salamon [10]).

We suppose that state-space is Hilbert space *X*, and input and output space are $U = R^m$ and $Y = R^p$, respectively, and that

– There exist two separable Hilbert space *V* and *W* with continuous, dense injection $W \subset X \subset V$ and that *A* generates a C_0-semigroup *S(t)* on *V*. It is consistent in the sense that restrictions of *S(t) to X* and *W* define C_0-semigroups, respectively, which are still written by *S(t)*. We further assume that $D_V(A) \subset W$, $D_{W^*}\left(A^*\right) \subset V^*$ where $D_V(A)$ denotes the domain of *A* considered as an operator on *V*.

– $B \in L(R^m, V)$ and for $u \in L_2(0, T, R^m)$ we have $\int_0^T S(T-s)Bu(s)ds_w \le b u_{L^2(0,T,R^m)}$.

– $E \in L(W, R^p)$ and for all $x \in W$ we have $E S(\cdot)x_{L^2(0,T,R^p)} \le g x_V$.

– There exist generalized transfer function $G(s)$ for $s \notin s(A)$ which satisfied the compatibility relationship for m, $s \notin s(A)$.

$G(s) - G(m) = (m-s)E(m-A)^{-1}(s-A)^{-1}B$ where $s(A)$. denotes the spectrum of the operator *A.* $G(s)$ is analytic and bounded in $Re\, s > a$, where a is the exponential growth rate of *S(t).*

Definition 1

a) We say that (*E, A, B*) is in a Pritchard-Salamon class if (s0) – (s2) hold.

b) We say that (*E, A, B*) is well-posedness in time and frequency domain on $[0, T]$ if (s0) – (s3) hold.

Callier-Desoer class (Callier and Desoer [11]).

Definition 2

a) For $m \in R^1$, we say that $f \in A(m)$ if

$$f(t) = \begin{cases} 0, \ t < 0; \\ f_a(t) + \sum_{i=0}^{\infty} f_i d(t - t_i), \text{ otherwise,} \end{cases} \tag{44}$$

where $f_a(t)\exp(-mt) \in L_1(0, \infty), t_i$ and f_i are real number, $0 = t_0 < t_1 < \dots, d$, represent the delta distribution, and $\sum_{i=0}^{\infty} |f_i| \exp(-mt) < q$.

b) We say that $f \in A_-(m)$ if there exist a $m_1 < m$ for which $f \in A(m_1)$.

c) $\hat{A}(m)$ and $\hat{A}_-(m)$ denote the classes of Laplace transform of $A(m)$ and $A_-(m)$, respectively.

d) $\hat{A}_-^{\infty}(m) = \{\hat{f} \in \hat{A}_-(m) \text{and } \hat{f} \text{ is bounded away from zero at } \infty \text{ in } C_m^+\}$ where $C_m^+ = \{s, Re\, s \ge m\}$, and $\hat{f}$ is bounded away from zero at ∞ in C_m^+ if there exist $h > 0$ and $r > 0$ such that $|\hat{f}(s)| \ge h$ for all $s \in C_m^+$ such that $|s - m| \ge r$.

e) $\hat{B}(m) = [\hat{A}_-(m)] \times [\hat{A}_-^{\infty}(m)]^{-1}$ is Callier-Desoer class.

f) $G(s) = [q_{ij}(s)]^{p \times m} \in \hat{B}(m)(\hat{A}_-(m))$ if $q_{ij}(s)$ are in $\hat{B}(m)(\hat{A}_-(m))$ for all i, j.

In the following procedure, we give the state-space and frequency domain descriptions of the non-slender flexible link, respectively. We choose $X = D(A_{1/2}) \oplus H$ as the state-space and the inner product of *X* is defined by

$$\begin{bmatrix} x_1 \\ x_2 \end{bmatrix}, \begin{bmatrix} y_1 \\ y_2 \end{bmatrix} H = x_1, y_{1\,H} + A^{1/2}x_1, A^{1/2}y_{1\,H} + x_2, y_{2\,H}, \tag{45}$$

where H is defined by (13) and $A^{1/2}$ is the square root operator of *A* given by (17). Since *A* is positive self-adjoint operator with the compact inverse on *H,* $A^{1/2}$ makes slues, and $D(A^{1/2}) \subset D(A)$.

Under the transformation $x^1 = u$, $x^1 = \dot{u}$, the dynamic system (19) with the output equation (43) is formally equivalent to

$$\dot{x} = Ax + Bf, y = Ex, \tag{46}$$

where $\left[x^1 x^2\right]^T$, and *A, B, E* are defined by

$$A = \begin{bmatrix} 0 & I \\ -A & -hA \end{bmatrix}, B = \begin{bmatrix} 0 \\ \Omega \end{bmatrix}, \tag{47}$$

$$E = \left[\Phi'(0)\ 0\right], f = \ddot{q}(t). \tag{48}$$

It is easy to see that *A* has eigenvalue m_n, $m_{-n}, n = 1,2,\ldots,$ given by

$$m_n, m_{-n} = -\frac{h}{2} l_n \pm g(l_n), \tag{49}$$

where l_n, $n = 1,2,\ldots$ are given by (37), and is defined by $g(l_n)$

$$g(l) = \begin{cases} \left(\frac{1}{4}h^2 l^2 - l\right)^{1/2}, \left(\frac{1}{4}h^2 l^2 - l\right) > 0; \\ i\left(l - \frac{1}{4}h^2 l^2\right)^{1/2}, \text{ otherwise.} \end{cases} \tag{50}$$

The normalized eigenvectors corresponding to m_n and m_{-n} are

$$\Psi_n = r_n \begin{bmatrix} \Psi_n \\ m_n \quad \Psi_n \end{bmatrix}, \qquad \Psi_{-n} = r_{-n} \begin{bmatrix} \Psi_n \\ m_{-n} \quad \Psi_n \end{bmatrix}, \tag{51}$$

where Ψ_n, $n = 1,2,\ldots$ are given by (39), (40) and

$$r_{\pm n} = \left(1 + l_n + |m_{\pm n}|^2\right)^{1/2}. \tag{52}$$

The eigenvectors of the adjoint operator A^* of *A* are

$$\Psi_n = \bar{r}_n \begin{bmatrix} \Psi_n \\ -\left(\frac{1 + l_n}{l_n}\right) m_n \Psi_n \end{bmatrix} \Psi_{-n}, \qquad \Psi_{-n} = \bar{r}_{-n} \begin{bmatrix} \Psi_n \\ -\left(\frac{1 + l_n}{l_n}\right) m_{-n} \Psi_n \end{bmatrix}, \tag{53}$$

where $\bar{r}_{\pm n}$ is taken as

$$\bar{r}_{\pm n} = \left(1 + l_n - |m_{\pm n}|^2 \left(\frac{1 + l_n}{l_n}\right)\right)^{-1} r_{\pm n}^{-1}, \tag{54}$$

such that $\{\Psi_n, \Psi_m\}$ forms a biorthogonal sequence in *X,* i.e.

$$\Psi_n, \Psi_{mX} = d_{mn} = \begin{cases} 1, & m = n; \\ 0, & m \neq n. \end{cases} \tag{55}$$

Let c^n, b^n be defined by

$$c^n = E\Psi_n, \quad b^n = B^* \Psi_n, \tag{56}$$

where B^* is the adjoint operator of *B* given by

$$B^* \begin{bmatrix} x^1 \\ x^2 \end{bmatrix} = x^2, \overset{\mathbf{r}}{\Omega}_H, \forall \begin{bmatrix} x^1 \\ x^2 \end{bmatrix} \in X. \tag{57}$$

For large values of *n*, using (42), we have the following useful estimations:

$$\left|c^n\right| = \Phi'_{|n|}(0)\, r_n = \begin{cases} 0(1), & n\ positive; \\ 0\left(n^{-1}\right), & n\ negative. \end{cases} \quad (58)$$

$$\left|b^n\right| = -\left(\frac{1+l_{|n|}}{l_{|n|}}\right) m_n\, \bar{r}_n \Psi_{|n|}, \overset{\mathbf{r}}{\Omega}_H = \begin{cases} 0\left(n^{-2}\right), & n\ positive; \\ 0\left(n^{-1}\right), & n\ negative. \end{cases} \quad (59)$$

$$\left|Re\, m_n\right| = \begin{cases} 0(1), & n\ positive; \\ 0\left(n^2\right), & n\ negative. \end{cases} \quad (60)$$

Using the estimations (58) – (60), it is easy to verify that

$$\sum_{n=-\infty}^{+\infty} \frac{\left|c^n\right|\left|b^n\right|}{\left|Re\, m_n\right|^a} < \infty, 0 \le a \le 1. \quad (61)$$

One may to prove that the state-space description (46) belongs to Pritchard-Salamon class, and has a well-defined transfer function *G(s)* given by

$$G(s) = \sum_{n=-\infty}^{\infty} \frac{c^n \bar{b}^n}{s - m_n}, \quad (62)$$

with the impulse response *h(t)*

$$h(t) = \sum_{n=-\infty}^{\infty} exp\left(m_n t\right) c^n \bar{b}^n.$$

The frequency domain description *G(s)* defined by (62) is in Callier-Desoer class $\hat{b}(o)$.

(*E, A, B*) subject to (46) is well posed.

Modal Control

As mentioned above, we see that the solution of the evolution equation (19) can be expressed as

$$u(t,x) = \sum_{n=1}^{\infty} u, \Psi_{nH}\, \Psi_n(t) = \sum_{n=1}^{\infty} \frac{1}{l_n} u_n(t) \Psi_n(t). \quad (63)$$

where $u_n(t) = Au, \Psi_{nH}$ is the solution of

$$\ddot{u}_n(t) + h\, l_n \dot{u}_n(t) + l_n u_n(t) = l_n \left\langle \Omega f, \Psi_n \right\rangle_H, \quad (64)$$

with the initial values $u_n(0) = Au_0, \Psi_{nH}$. and $\dot{u}_n(0) = l_n \left\langle u_{to}, \Psi_n \right\rangle_H$,

where u_0, u_{to} are the initial values of the system (19).

Using the coordinate system based on an orthonormal basis $\left\{\Psi_n\right\}_{n=1}^{\infty}$, we may represent $u = \left[u_1, u_2 \ldots u_n \ldots\right]^T$ $A = diag\left[l_1, l_2 \ldots\right]$. Let $x_n = \left[x_n^1\ x_n^1\right]^T = \left[u_n\ \dot{u}_n\right]$. We rearrange the state $\left[u^T\ \dot{u}^T\right]^T$ as $\left[x_1^T\ x_2^1 \ldots\right]^T$, where x_n satisfies

$$\dot{x}_n = \begin{bmatrix} 0 & 1 \\ -l_n & -h\, l_n \end{bmatrix} x_n + \begin{bmatrix} 0 \\ l_n \Omega, \Psi_{nH} \end{bmatrix} f. \quad (65)$$

Taking $x_n = T_n \bar{Z}_n$, T_n is given by

$$T_n = \begin{bmatrix} \frac{1}{2} & \frac{1}{2} \\ \frac{1}{2} m_n & \frac{1}{2} m_{-n} \end{bmatrix}, n = 1, 2, \ldots$$

Then above transformation carries (65) into

$$\dot{\bar{Z}}_n = \begin{bmatrix} m_n & 0 \\ 0 & m_{-n} \end{bmatrix} \bar{Z}_n + \begin{bmatrix} 1 \\ -1 \end{bmatrix} l_n g^{-1}(l_n) \langle \Omega, \Psi_n \rangle_H \, f . \tag{66}$$

Since $g^2(l)$ is strictly increased with respect to l, there exist a n_0 such that

$$g(l_n) = \begin{cases} g_n, \; n > n_0; \\ i\bar{g}_n, n \le n_0, \end{cases} \tag{67}$$

where $\bar{g}_n = \left(l_n - \frac{1}{4} h^2 l_n^2 \right)^{1/2}$ and $g_n = \left(\frac{1}{4} h^2 l_n^2 - l_n \right)^{1/2}$ are real numbers.

As $n \le n_0$, $\bar{Z}_n^1$, and $\bar{Z}_n^2$ are complex conjugates. Thus taking

$$Z_n^1 = \begin{cases} \frac{1}{2}\left(\bar{Z}_n^1 + \bar{Z}_n^2 \right), n \le n_0; \\ \bar{Z}_n^1, \; n > n_0. \end{cases} \tag{68}$$

$$Z_n^2 = \begin{cases} i\left(\bar{Z}_n^2 - \bar{Z}_n^1 \right), \; n \le n_0; \\ \bar{Z}_n^2, \; n > n_0, \; i^2 = -1, \end{cases} \tag{69}$$

then $Z = \left[Z_1^T \;\; Z_1^T \; \dots \right]^T$ satisfies

$$\dot{Z} = AZ + Bf, \;\; y = C \cdot Z , \tag{70}$$

where *A, B, C* are defined by $A = \text{blog diag}\left[A_1, A_2, \dots \right]$, $B = \left[B_1^T, B_2^T \; \dots \right]^T$, $C = \left[C_1, C_2, \dots \right]$ and for every *n* (*n=1, 2,…*)

$$A_n = \begin{cases} \begin{bmatrix} -\frac{1}{2} h\, l_n & -\bar{g}_n \\ \bar{g}_n & -\frac{1}{2} h\, l_n \end{bmatrix}, n \le n_0. \\ \begin{bmatrix} m_n & 0 \\ 0 & m_{-n} \end{bmatrix}, n > n_0, \end{cases} \tag{71}$$

$$B_n = \begin{cases} \frac{l_n}{\bar{g}_n} \langle \Omega, \Psi_n \rangle_H \begin{bmatrix} 0 \\ 1 \end{bmatrix}, \; n \le n_0; \\ \frac{l_n}{\bar{g}_n} \langle \Omega, \Psi_n \rangle_H \begin{bmatrix} 1 \\ -1 \end{bmatrix}, \; n > n_0. \end{cases} \tag{72}$$

$$C_n = \begin{cases} \left[\frac{\Phi_n'(0)}{l_n}, \; 0 \right], n \le n_0; \\ \left[\frac{\Phi_n'(0)}{2 l_n}, \; \frac{\Phi_n'(0)}{2 l_n} \right], n > n_0. \end{cases} \tag{73}$$

Taking $\tilde{Z} = \left[q \;\; \dot{q} \;\; Z^T \right]^T$, the modal state-space equation of the flexible link is expressed by

$$\Sigma_1 : \dot{\tilde{Z}} = \tilde{A}\tilde{Z} + \tilde{B}f, \;\; \tilde{y} = \tilde{C} \cdot \tilde{Z} , \tag{74}$$

where $\tilde{y} = \left[q \ \dot{q}_y \right]^T$ and

$$\tilde{A} = \begin{bmatrix} 0 & 1 & 0 \\ 0 & 0 & 0 \\ 0 & 0 & A \end{bmatrix}, \tilde{B} = \begin{bmatrix} 0 \\ 1 \\ B \end{bmatrix}, \tilde{C} = \begin{bmatrix} 1 & 0 & 0 \\ 0 & 1 & 0 \\ 0 & 0 & C \end{bmatrix}.$$

We introduce the following notation:

$$\tilde{A}^n = \begin{bmatrix} 0 & 1 & 0 \\ 0 & 0 & 0 \\ 0 & 0 & A^n \end{bmatrix}, \tilde{B}^n = \begin{bmatrix} 0 \\ 1 \\ B^n \end{bmatrix}, \tilde{C}^n = \begin{bmatrix} 1 & 0 & 0 \\ 0 & 1 & 0 \\ 0 & 0 & C^n \end{bmatrix},$$

where A^n, B^n, C^n are defined by

$$\begin{cases} A^n = blog\,diag\left[A_1, A_2, \ldots, A_n\right]; \\ B^n = \left[B_1^T, B_2^T \ldots B_n^T \right]^T; \\ C^n = \left[C_1, C_2, \ldots C_n\right]. \end{cases} \tag{75}$$

Then using this notation, in view of (74), we obtain the (2n+2) – dimensional approximation system of Σ_1.

$$\Sigma_2 : \dot{\tilde{Z}}^n = \tilde{A}^n \tilde{Z}^n + \tilde{B}^n f \; \tilde{y}^n = \tilde{C}^n \cdot \tilde{Z}^n . \tag{76}$$

In what follows, the feedback controller is designed based on *n*-modal state-space equation Σ_2 in the customary way.

In practice, b is usually small compared with a , thus we have good reason to assume

$$a \neq b , \tag{77}$$

where a , b are defined by (25).

The conditions for controllability and observability of the system Σ_2 are presented next; these are required for the design of compensator.

One may to proof that (A^n, B^n, C^n) is controllable and observable if

$$\Phi_i'(0) \neq 0, \; i = 1, 2 \ldots n . \tag{78}$$

$\tilde{A}^n$, $\tilde{B}^n, \tilde{C}^n$ is controllable and observable if the conditions in (78) hold.

Using (40) and the assumption (77), we see that it is easy to verify that the conditions in (78) hold for all *i*.

The design of the compensator is in two parts:

a) Constructing the estimator of modal state Z^n. We take the Luenberger observer [12] of Z^n as

$$\dot{\hat{Z}}^n = \left[A^n - G^n C^n \right] \hat{Z}^n + \tilde{G}^n \tilde{y} + B^n f , \tag{79}$$

where G^n is the estimator gain selected in such way that the spectrum of matrix $A^n - G^n C^n$ lies to the left of a vertical line $Re\, s = -s$, and $s > 0$ can prescribed by the investigator because (C^n, A^n) is observable and $\tilde{G}^n = \left[0 \ 0 \ G^n \right]$. Using the information of output $\tilde{y}$, the estimator (79) produces the estimate $\hat{Z}^n$ of Z^n.

b) Designed the feedback control law. The form of the feedback control scheme is taken as

$$f(t) = k_1 q + k_2 \dot{q} + k_3 \hat{Z}^n . \tag{80}$$

Let $\tilde{K} = [k_1\, k_2\, k_3]^T$ denote the feedback gain that can be determined by the pole allocation method or the steady-state optimal regulator method.

(i) Pole allocation method [12]. In this case, the feedback control gain can be chosen in such way that the eigenvalues of $\hat{A}^n + \hat{B}^n \tilde{K}$ lie to the left of a vertical line $Re\, s = -s$ because ($\tilde{A}^n, \tilde{B}^n$) is controllable.

(ii) Optimal regulator method [13]. In order to suppress the tip vibrations, the form of the performance index is taken as

$$I(f) = \int_0^\infty \left\{ \begin{array}{l} q_1 w^2(t,l) + q_2 \dot{w}^2(t,l) + q_3 \Phi^2(t,l) + q_4 \dot{q}^2(t,l) + q_5 q^2 + q_6 \dot{q}^2 + \\ + r_1 f^2(t) \end{array} \right\} exp(2s\, t)\, dt, \tag{81}$$

Using the expression (63), (64), *I(f)* can be rewritten as $I(f) = \int_0^\infty \left\{ \tilde{Z}^{nT} Q\, \tilde{Z}^n + r_1 f^2(t) \right\} exp(2s\, t)\, dt$.

Then the feedback gain $\tilde{K}$ is determined by solving the Ricatti equation.

In summary, the finite dimensional feedback controller can be formally formulated by

$$\Sigma_3 : \begin{cases} \dot{\hat{Z}}^n = \left[A^n - G^n C^n \right] \hat{Z}^n + \hat{G}^n \tilde{y} + B^n f; \\ f(t) = k_3 \hat{Z}^n + \bar{K}\tilde{y}, \ \bar{K} = [k_1, k_2, 0]. \end{cases} \tag{82}$$

Let $q_d(t)$ and $\dot{q}_d(t)$ be given desired rotation angle and angular velocity of the motor, respectively.

Then the closed-loop configuration of the control system can be illustrated by Fig. 2, in which $v_d = k_1 q_d + k_2 \dot{q}_d$ and v_0 is observation noise.

If the rotation motor is an armature-controlled dc-motor with negligible armature inductance, then

$$V_a(t) = R_q i_a(t) + l_b, \ t(t) = k_a i_a(t), \tag{83}$$

where k_a is known as the motor torque proportional constant, i_a, R_a, V_a are armature current, resistance and voltage, respectively (see Fig. 3, *a*). l_b is the back electromotive force which is proportional to the angular velocity of the motor, i.e.:

$$l_b = k_b \dot{q}, \tag{84}$$

where k_b is a proportional constant.

Combination of (9), (12), (80), (83) and (84) gives the following feedback control law

$$V_a = \frac{R_a}{k_a}(I_m + I_h)\dot{\tilde{f}} + m\left(\int_0^t \tilde{f} dt + \dot{q}(0) \right) - EIy - h\, EI\dot{y} + k_b \left(\int_0^t \tilde{f} dt + \dot{q}(0) \right), \tag{85}$$

where $\tilde{f} = f - v_d$, and $\dot{q} - v_d$, and $\dot{q}$ and y are known.

The structure of the overall control system is show in Fig. 3, *b*.

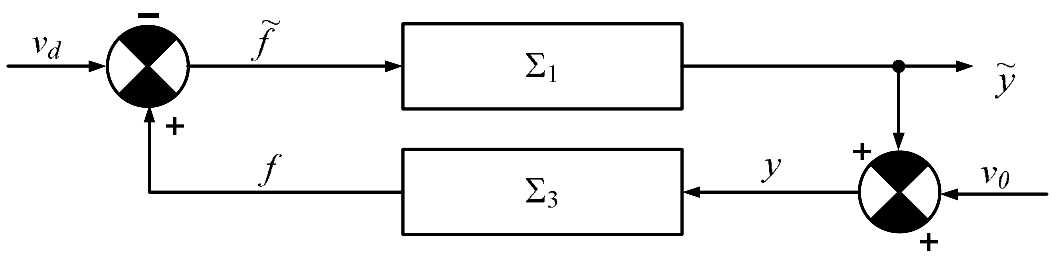

Fig. 2. *Closed-loop configuration of a control system*

Stabilization

Firstly, we recall the definition of stabilization for the Pritchard-Salamon system [14].

Definition 3.

We assume that (*E, A, B*) is a Pritchard-Salamon system, which satisfies (s0) – (s3) in Definition 5.1, and *s(t)* is a C_0-semigroup generated by *A*, *G(s)* is the well-defined transfer function of (*E*, *A*, *B*). Then

a) (*E, A, B*) is said to be s -exponentially stable if *S(t)* is exponentially stable with decay rate exceeding s .

b) (*A, B*) is said to be s -exponentially stabilizable on *W* if there exist an operator $K \in L\left(W, R^m\right)$ such that the perturbed $[A + BK]$-semigroup $S_K(t)$ is s -exponentially stable on *W*.

c) (*E, A*) is said to be s -exponentially detectable on *V* if there exists an operator $L \in L\left(R^p, V\right)$ such that the perturbed $[A + LK]$-semigroup $S_L(t)$ is s -exponentially stable on *V*.

d) (*E, A, B*) is said to be s -input-output stable if the system transfer function *G(s)* $G(s) \in \hat{A}\_(s)$.

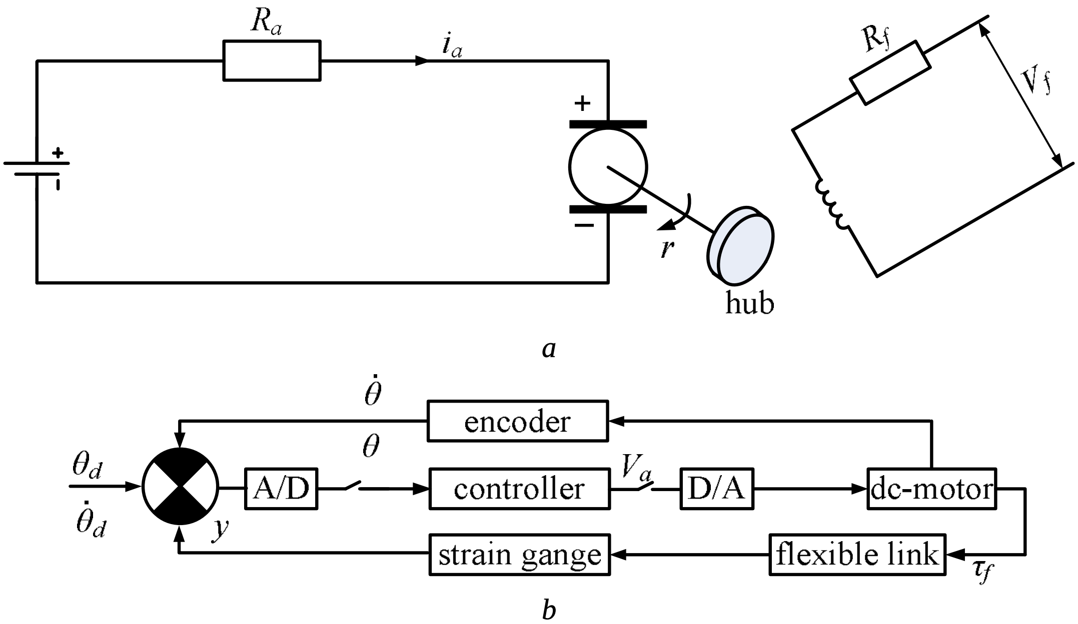

Fig. 3. *Equivalent circuit of a dc-motor (a); the overall system block diagram (b)*

Consider the *n*-modal control system Σ_2 controlled by the controlled by the controller Σ_3; the closed-loop structure is shown in the Fig. 4, *a*.

We introduce the new state $X_c^n = \left[\hat{Z}^{nT}, e^{nT}\right]^T$, where $e^n = \hat{Z}^n - Z^n$; then the closed-loop state equation can be rewritten as $\dot{X}_c^n = A_c X_c^n + B_c v_c$, $y_c = C_c X_c^n + v_c$ where $v_c == \left[v_d^T, v_o^T\right]^T$, $\left[y_c = \left[\bar{y}^{nT}, \hat{f}\right]\right]$, and

$$\begin{cases} A_c = \begin{bmatrix} \tilde{A}^n + \tilde{B}^n \tilde{K}; & \tilde{B}^n k_3; \\ 0; & A^n - G^n C^n \end{bmatrix}, \\ B_c = \begin{bmatrix} \tilde{B}^n & 0 \\ 0 & \tilde{G}^n \end{bmatrix}, C_c = \begin{bmatrix} \tilde{C}^n & 0 \\ \tilde{K} & k_3 \end{bmatrix}. \end{cases} \tag{86}$$

From the expression of A_c in (86), we see that the eigenvalues of the operator A_c are

$$s\left(A_c\right) = s\left(\breve{A}^n + \breve{B}^n\breve{K}\right) \cup s\left(A^n - G^nC^n\right). \tag{87}$$

It may be proved that the closed-loop system (Σ_2, Σ_3) shown in the Fig. 4, *a* s-exponentially stable as well as s-input-output stable.

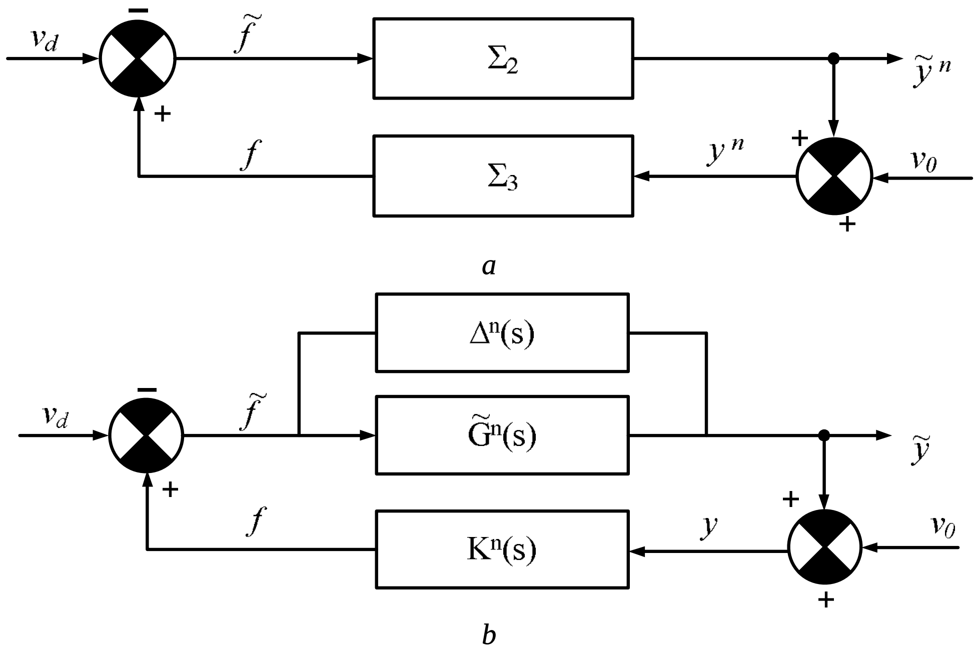

Fig. 4. *Closed-loop configuration of a finite dimensional approximation control system (a); the illustration of a perturbation feedback (b)*

One may be to imply that the compensator Σ_3 can stabilize the ***n***-modal control system Σ_2 in the sluse of σ-exponentially stable. For application, we hope that the controller Σ_3 can also stabilize the original control system Σ_1 in the same sense. In what follows, we focus on the non-slender flexible link system Σ_1?

From the above discussion, we see that $(\mathring{C}, \mathring{A}, \mathring{B})$ is also a Pritchard-Salamon system and has transfer function $\mathring{G}(s)$ which is in Callier-Desoer class, expressed as

$$\breve{G}(s) = \begin{bmatrix} G_q \\ G(s) \end{bmatrix}, G_q(s) = \begin{bmatrix} \frac{1}{s^2} \\ \frac{1}{s} \end{bmatrix}. \tag{88}$$

Let $G^n(s)$ be the transfer function of (C^n, A^n, B^n) expressed as

$$G^n(s) = \sum_{i=-n}^{n} \frac{c^i \bar{b}^i}{s - m_i}. \tag{89}$$

Consequently, the transfer function of Σ_2 is

$$\breve{G}^n(s) = \begin{bmatrix} G_q(s) \\ G^n(s) \end{bmatrix}., \tag{90}$$

The transfer function of Σ_3, $K^n(s)$, can be expressed as

$$K^n(s) = \left[I - k_3\left(sI - A^n + G^nC^n\right)^{-1} B^n\right]^{-1}\left[k_3\left(sI - A^n + G^nC^n\right)^{-1} \tilde{B}^n + \tilde{K}\right]. \qquad (91)$$

Let $\Delta^n(s)$ denote the residual term defined by

$$\Delta^n(s) = \begin{bmatrix} 0 \\ G(s) - G^n(s) \end{bmatrix}. \qquad (92)$$

In Fig. 4, *b*, we view the system Σ_1 as the result from system Σ_2 perturbed by the term $\Delta^n(s)$. In the following discussion, we assume that

$$s \neq \frac{h}{2} l_n, n = 1,2,\ldots, \frac{h}{2} l_1 < s < \frac{1}{h}. \qquad (93)$$

One may to prove that the closed-loop system shown in Fig.4(b) s -input-output stable if and only if

$$\left\|\Delta^n(s)\right\|_\infty < \left(\left\|K^n(s)\left[I - \tilde{G}(s)K^n(s)\right]^{-1}\right\|_\infty\right)^{-1}, \qquad (94)$$

where $\|\bullet\|_\infty.$ is the L_∞-norm, defined by

$$\|G\|_\infty .= sup_\Omega \left\|G(j\Omega)\right\|_2, \qquad (95)$$

and $\|M\|_2$ is the largest singular value of *M*.

The closed-loop system shown in Fig. 2 is s -exponentially stable if and only if condition (94) holds, as well.

Computer simulation

Here the non-slender flexible link is assumed to be made of aluminium. The experimental parameters used in our simulation are:

$L = 1,27\,m,\ A = (3,2 \times 4,0) \times 10^{-5}\,m^2,\ I = 1,092 \times 10^{-10}\,m^4,$

$C = 2,1067 \times 10^6\,N,\ E = 7,11 \times 10^{10}\,N/m^2,\ r = 3,475 \times 10^{-1}\,kg/m,$

$M = 62,0 \times 10^{-3}\,kg,\ I_h = 0,03\ kg \cdot m^2,\ I_m = 0,005\ kg \cdot m^2,\ m = h = 0,002.$

By solving the characteristic equations (35), we obtain the eigenvalues. Consequently, eigenvectors can be calculated by the formulae (39), (40). In our simulation, the flexible link is approximated by the first five modes, and the controller is designed based on the first three modes. l_i, $m_{\pm i}$, and $\Phi_i'(0)(i = 1,2,\ldots 5)$ are listed in the Table.

Table

Modal parameters for first five flexible modes

n	λ_n	***Re*** μ_n	***Im*** $\mu_n = \bar{g}_n$	Φ_n'
1	$6{,}77 \cdot 10^1$	$-6{,}77 \cdot 10^{-2}$	$8{,}77 \cdot 10^0$	$-3{,}05 \cdot 10^0$
2	$3{,}03 \cdot 10^3$	$-3{,}03 \cdot 10^0$	$5{,}50 \cdot 10^1$	$-2{,}54 \cdot 10^1$
3	$2{,}55 \cdot 10^4$	$-2{,}55 \cdot 10^1$	$1{,}58 \cdot 10^2$	$-8{,}24 \cdot 10^1$
4	$1{,}03 \cdot 10^5$	$-1{,}03 \cdot 10^2$	$3{,}04 \cdot 10^2$	$-1{,}76 \cdot 10^2$
5	$2{,}90 \cdot 10^5$	$-2{,}90 \cdot 10^2$	$4{,}45 \cdot 10^2$	$-3{,}09 \cdot 10^2$

That $a = 2,2856 \times 10^{-6}$ and $b = 5,2907 \times 10^{-7}$ implies that $\Phi_i'(0) \neq 0$ for any *i*, which guarantees the controllability and the observability of the system (C_i, A_i, B_i) for any *i*. In our simulation, the feedback gain $\tilde{K}$ is determined by the $L\ Q\ R$ method, and the weighting parameters are $q_1 = q_2 = q_3 = q_4 = 130$, $q_5 = q_6 = 100$, $r_1 = 1$, $s = 3$. Observing the Table and the experimental parameters, we see that assumption (93) holds, and condition (94) can be easily verified by the following simply calculations: $\left\| K^n \left(I - \hat{G}^n K^n \right) \right\|_\infty^{-1} = 6,0362 \times 10^{-4}$ and $\left\| \Delta^n \right\|_\infty = 4,7509 \times 10^{-5}$. These imply that the controller can stabilize the non-slender flexible link.

The initial values are assumed to be $u_0 = u_{t0} = 0$, and the desired rotation angle $q_d(t) = 60^\circ$ and $\dot{q}_d = 0$. The transient responses of the tip displacement *w(t, l),* tip slop arising from bending $\Phi(t,l)$, the motor rotation angle q, the angular velocity $\dot{q}$ and the corresponding torque supplied by the motor are shown in Fig. 5, *a–e*, while the same transient responses and the torque are shown in Fig. 6 in the case where $k_3 = 0$. The simulation results give good proof of the validity of our results.

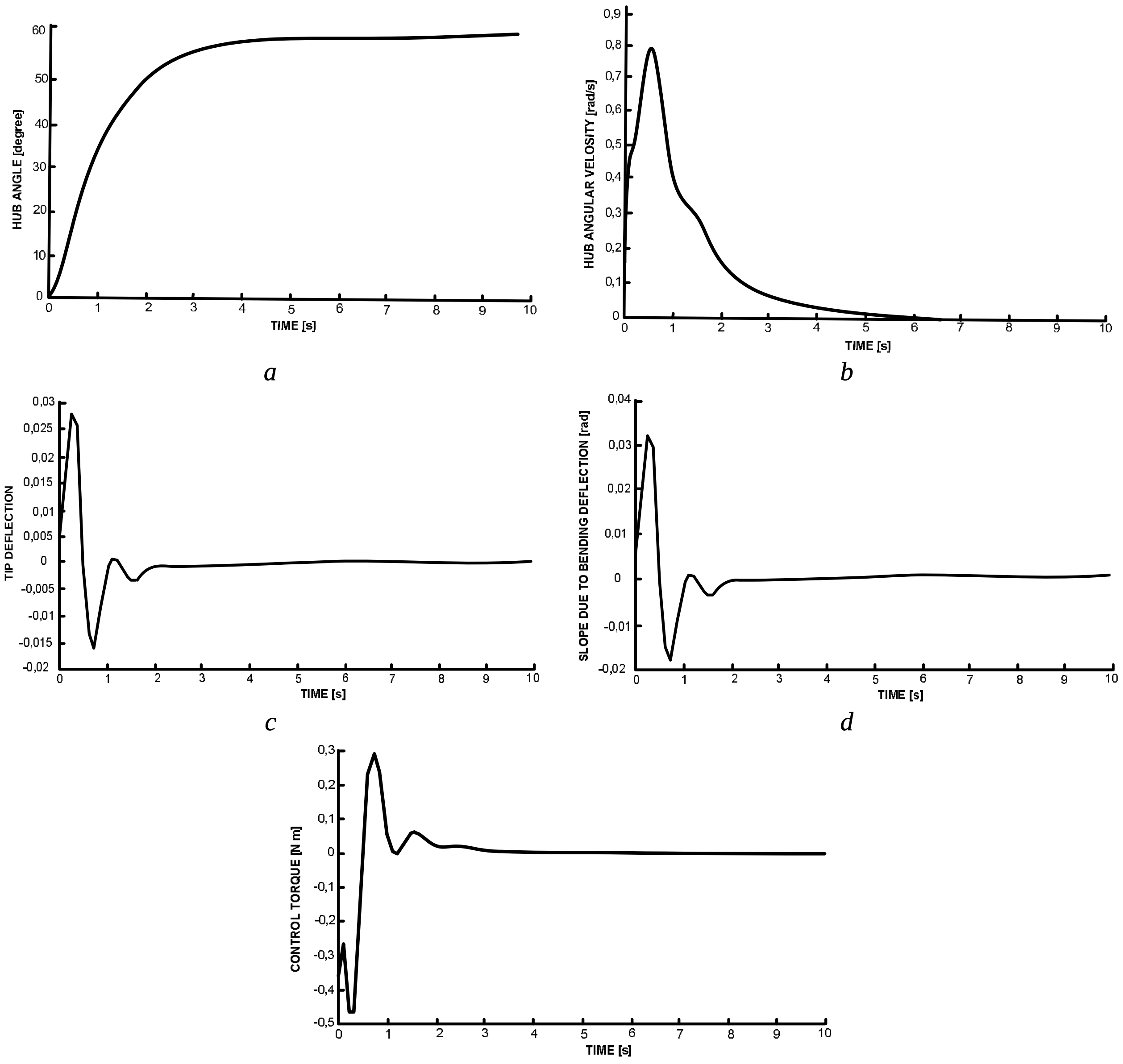

a *b* *c* *d* *e*

Fig. 5. *(a) Hub angle with flexibility feedback; (b) hub angular velocity with flexibility feedback; (c) tip deflection with flexibility feedback; (d) slope due to bending deflection at tip deflection with flexibility feedback; (e) control torque applied to link with flexibility feedback*

Conclusions

In this paper we have given an analytical study on the modelling and control of single non-slender flexible links. Our results are as follows:

a) By Hamilton's principle, it was shown that the elastic motion of the non-slender flexible link governed by a pair of coupled partial differential equations with coupled boundary conditions.

b) Using spectral analysis, we showed that the dynamic control system has a well-posed state-space description (Salamon class) as well as well-defined transfer function belonging to Callier-Desoer class.

c) The feedback modal control scheme was presented. An easily checkable condition that is sufficient and the necessary for the stabilization of the closed-loop control system was given. The results of a computer simulation study were presented to illustrate our results.

Although in our present study, the dynamic equation is necessary for modelling and control of single non-slender flexible links, it is more complex than that of slender flexible links, and its computational cost is so high that it is not necessary for the slender case. Thus, it is of interest to note how to identify whether a flexible links is slender. This will be presented elsewhere.

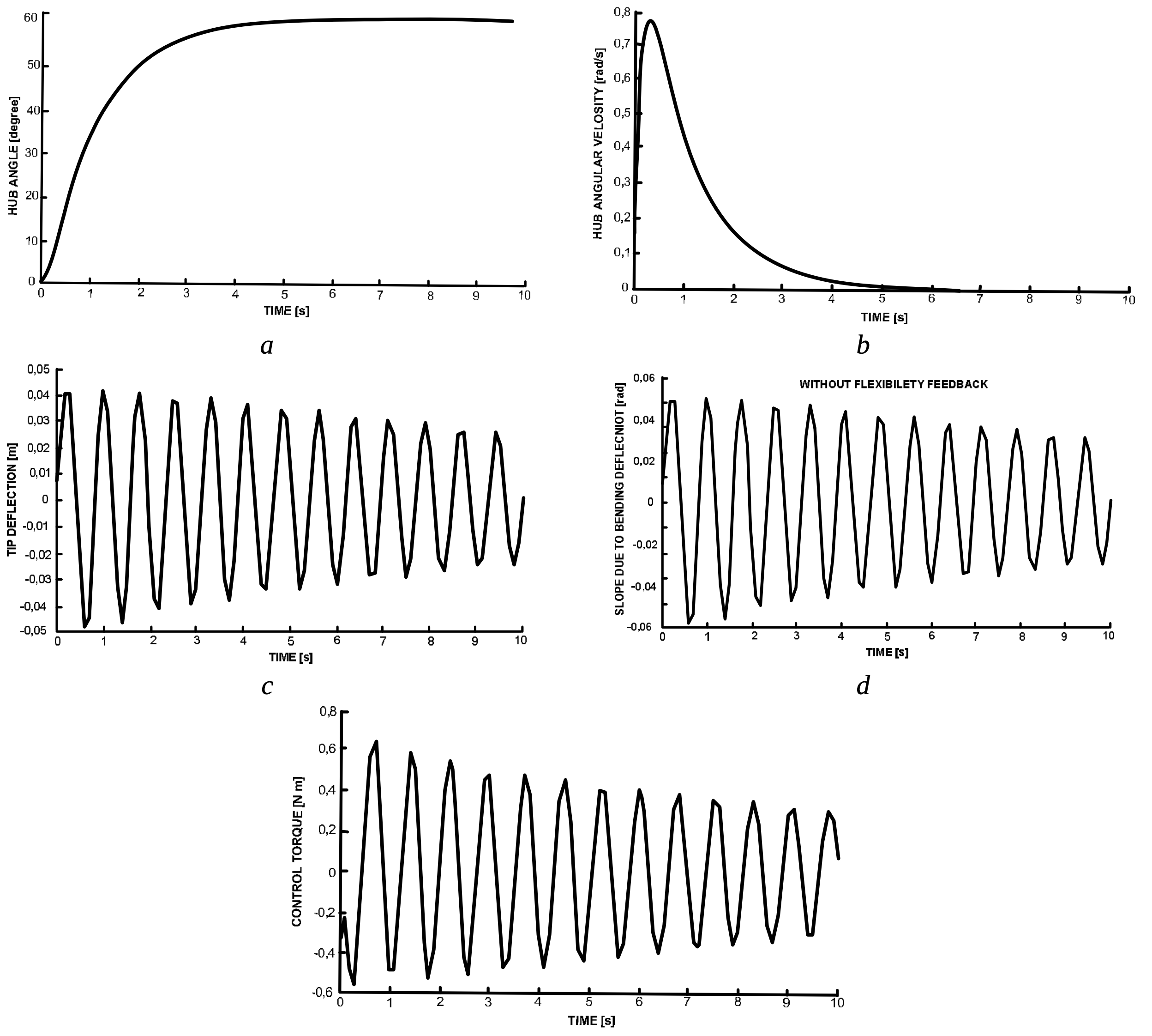

e

Fig. 6. *Hub angle without flexibility feedback (a); hub angular velocity without flexibility feedback (b); tip deflection without flexibility feedback (c); slope due to bending deflection at tip deflection without flexibility feedback (d); control torque applied to link without flexibility feedback (e)*

References

[1] Tzafestas S., Kanoh H. Proc. IMAC/IFAC Symp. on Modelling and Simulation of DPS, Japan, 1987. – 267 p.

[2] Fukuda T., et al. // J. Robot. Mech. – 1989. – Vol. 1. – 12 p.

[3] Sakawa Y., et al. // J. Robot. Systems. – 1985. – Vol. 2. – 453 p.

[4] Barbier E., Özüner Ü //ASME J. Dynam. Systems. Meas. Control. – 1988. – Vol. 110. – 416 p.

[5] Timoshenko S. Vibration Problems in Engineering. – New York: Van Nostrand, 1955. – 400 p.

[6] Traill-Nash R. W., Collar A. R. // Quart. J. Mech. Apple. Math. – 1953. – Vol. 4. – 186 p.

[7] Bayo E., et al. // Int. J. Robot. Autom. – 1988. – Vol. 3. – 150 p.

[8] Bayo E. // Int. J. Robot. Autom. – 1989. – Vol. 4. – 53 p.

[9] Wang G. L., Lu G. Z. Technical Report, Robotic Research Laboratory, Nankai University, People's Republic of China. – 1990. – 100 p.

[10] Pritchard A. J., Salamon D // J. Control Optim. – 1987. – Vol. 25. – 121 p.

[11] Callier F. M., Desoer C. A. // Am. Soc. Sci. – 1980. – Vol. 94. – 7 p.

[12] Luenberger D. G. //IEEE Trans. Autom. Control. – 1971. – Vol. 16. – 596 p.

[13] Anderson B. D. O. Linear Optimal Control / B. D. O. Anderson, I. B. Moore. – Englewood Cliffs, N.J.: Prentice-Hall, 1970.

[14] Curtain R. F. Infinite Dimensional Linear System Theory. Lecture Notes in Computer Science / R. F. Curtain, A. J. Pritchard. – Berlin: Springer-Verlag, 1978. – 8 p.